SUPPLEMENTAL FIGURES S1

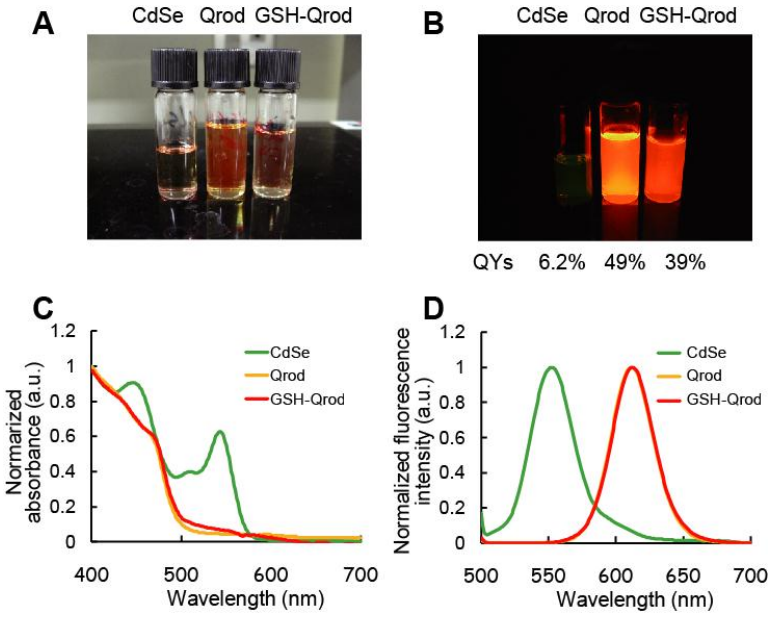

Figure S1. Glutathione coated Qrod emissions at 612 nm. (**A, B**) Non-fluorescent (**A**) and fluorescent (**B**) images of CdSe, Qrods and GSH-Qrods. (**C, D**) Normalized absorbance (**C**) and fluorescence (**D**) spectra of CdSe (green), Qrods (yellow) and GSH-Qrods (red). The width and length of the Qrods were 8.1 ± 3.1 nm and 41.9 ± 7.1 nm, respectively.

SUPPLEMENTAL FIGURES S2-3

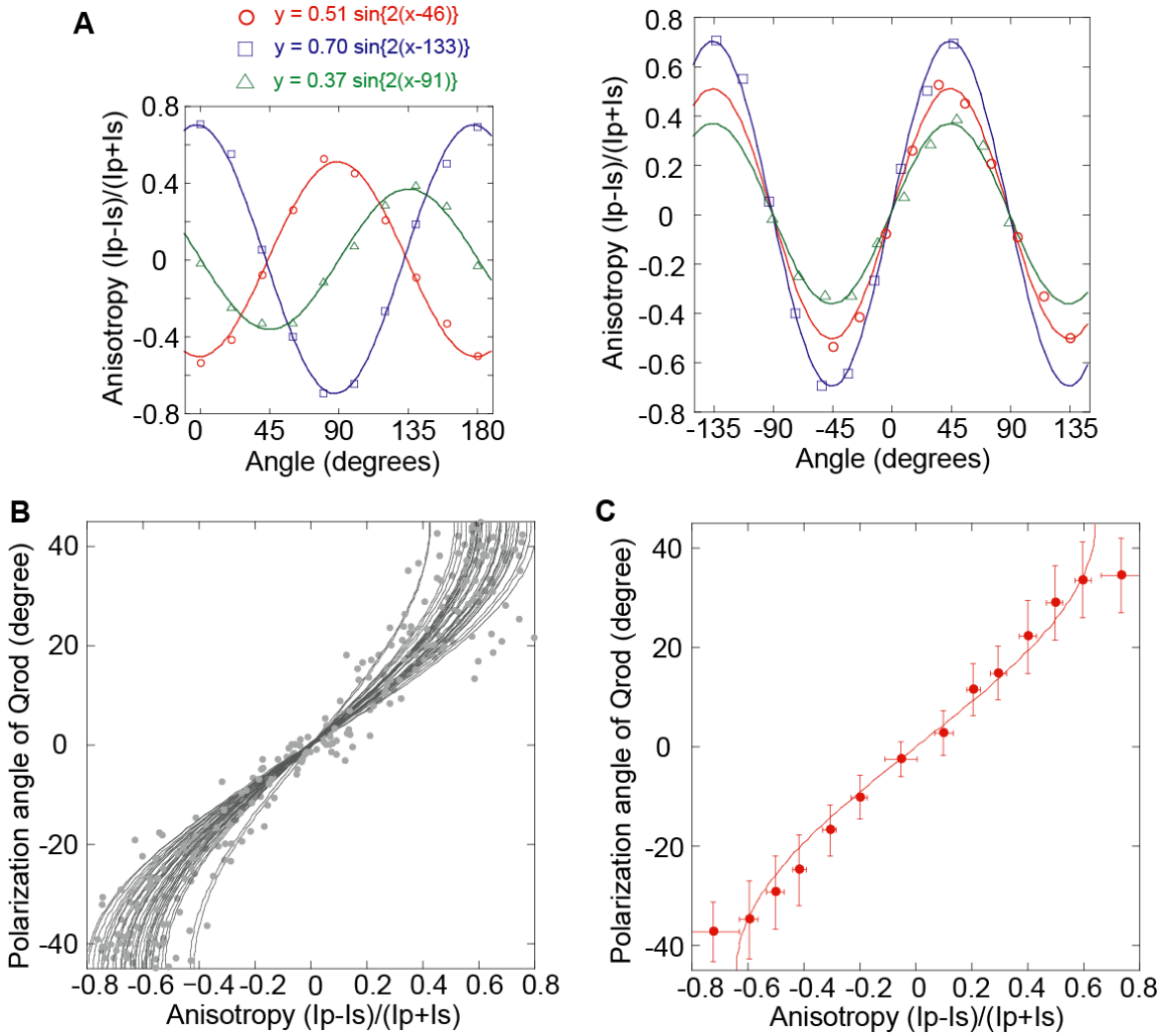

Figure S2. Calibration curve of anisotropy and angle of Qrods. (**A**) *Left*, Typical traces of anisotropy of single GSH-Qrod as a function of the rotation angle of the 1/2λ wave plate. Color indicates each Qrod. The solid lines are the data fits with a sine function ($y = a_1 \cdot \sin\{2 \cdot (x-a_2)\}$). *Right*, the results of the adjustment of the phase with the fitting parameter of a_2. (**B**) Distribution of relationship between anisotropy and angle of individual Qrods (N = 38). Solids lines are the fitting results of each plot with an arcsine function. Each solid line is used as a calibration curve for individual Qrods. (**C**) Unified calibration curve of anisotropy and angle of Qrods using all Qrod data (N = 38). Error bars are standard deviations. Solid line is the fitting result with an arcsine function.

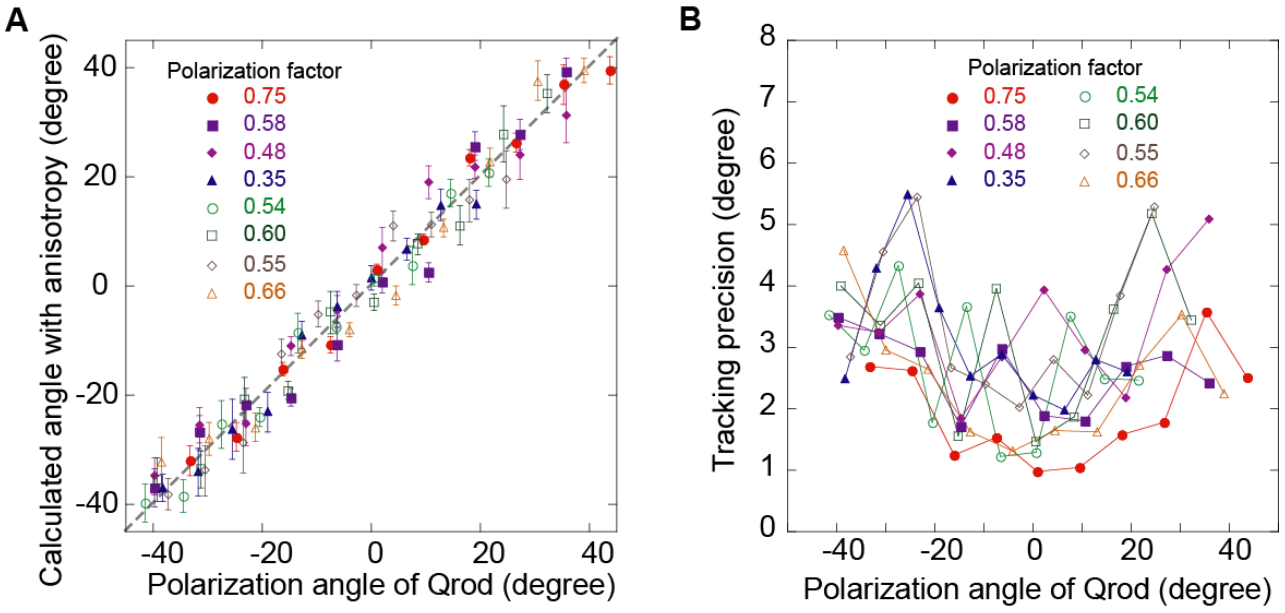

Figure S3. Conversion precision and angular tracking precision of Qrods. (**A**) Relationship between angles calculated from each calibration curves and actual polarization angle of Qrods. A Qrod was fixed on the coverslip and the polarization angle was changed by rotating a phase plate located before the imaging lens. The apparent angle of the same Qrod was calculated using the calibration curve between polarization angles and anisotropy. The anisotropic image was obtained for 3 s with 30 frames/sec (100 images). Error bars are the standard deviation of 100 data points. 8 typical polarization factors are shown. Colors indicate different Qrods with each polarization factor. (**B**) Relationship between the angular tracking precision and polarization angle of Qrods. The tracking precision was determined as the standard deviation of 100 data points (see error bars in S3A). Eight typical polarization factors are shown. Colors indicate different Qrods with each polarization factor.

SUPPLEMENTAL FIGURES S4-5

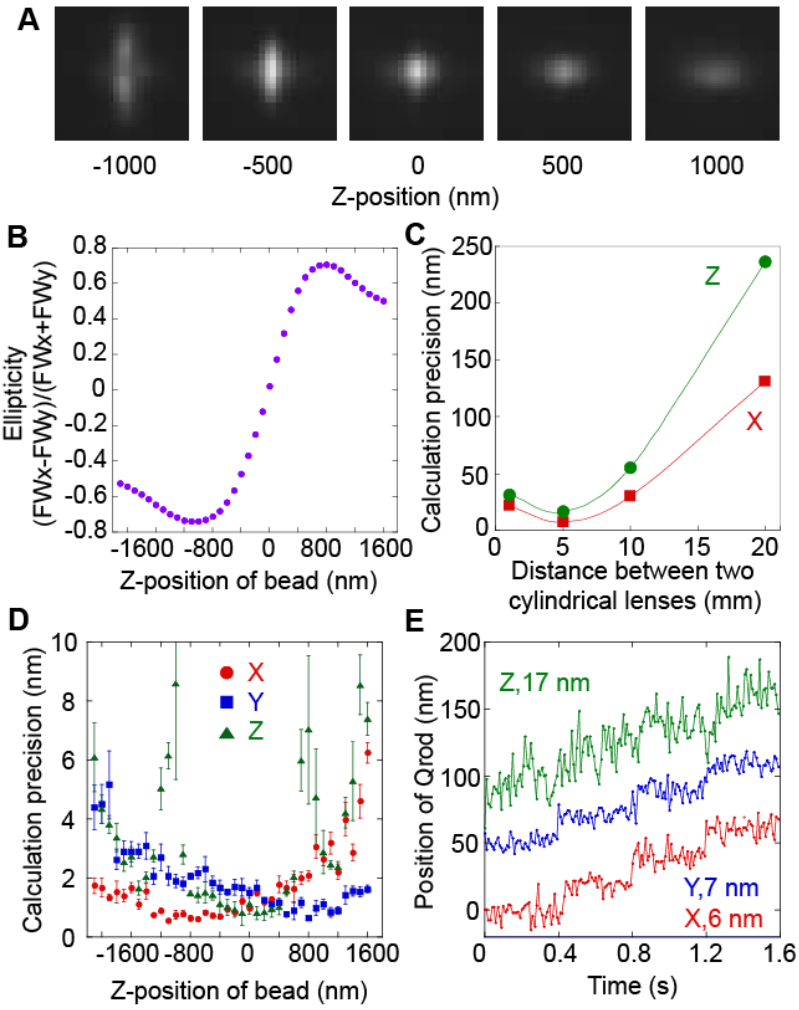

Figure S4. Optimization of 3D single particle tracking. (**A**) Fluorescent images of a single fluorescent bead with a diameter of 100 nm at various Z-positions (-1000 to 1000 nm). (**B**) Ellipticity of a single fluorescent bead image as a function of the Z-position (-2200 to 1800 nm). (**C**) Calculation of the precision in the X- (red) and Z-directions (green) as a function of distance between CvC and CnC, the two cylindrical lenses in the optics system (Fig.1). The precision was defined using the standard deviation of 100 X- or Z-positions calculated by fitting the image with a 2D ellipsoidal Gaussian function. The Z-position of the beads was near zero. The tracking precision depended on the astigmatism, and the optimal distance between CnC and CvC was 5 mm. (**D**) Calculated precision in the X-, Y-, and Z-directions (red, blue, and green symbols, respectively) as a function of Z-position when the camera received 15,000 photons from a fluorophore. The 3D tracking precisions was 2 nm in the X- and Y-axes and 5 nm along the Z-axis. The calculated Z-axis precision depended on the position, and had a reliable range between -800 and 800 nm. Error bars represent standard deviations of 20 data. (**E**) Test tracking with 20 nm stepping when the two cylindrical lenses were separated 5 mm, the Z–position of the Qrod was near zero, and the CCD camera received 1,500 photons per frame from a GSH-Qrod. The GSH-Qrod fixed on a coverslip was moved by discrete 20 nm steps every 0.4 s in the X- (red line), Y- (blue line) and Z-axes (green line) simultaneously using two Piezo actuators. The frame rate of the CCD camera was 100 frames/sec. Standard deviations of the tracking for 2 sec excepting the stepping moments were 6, 7 and 17 nm in the X-, Y- and Z-axes, respectively.

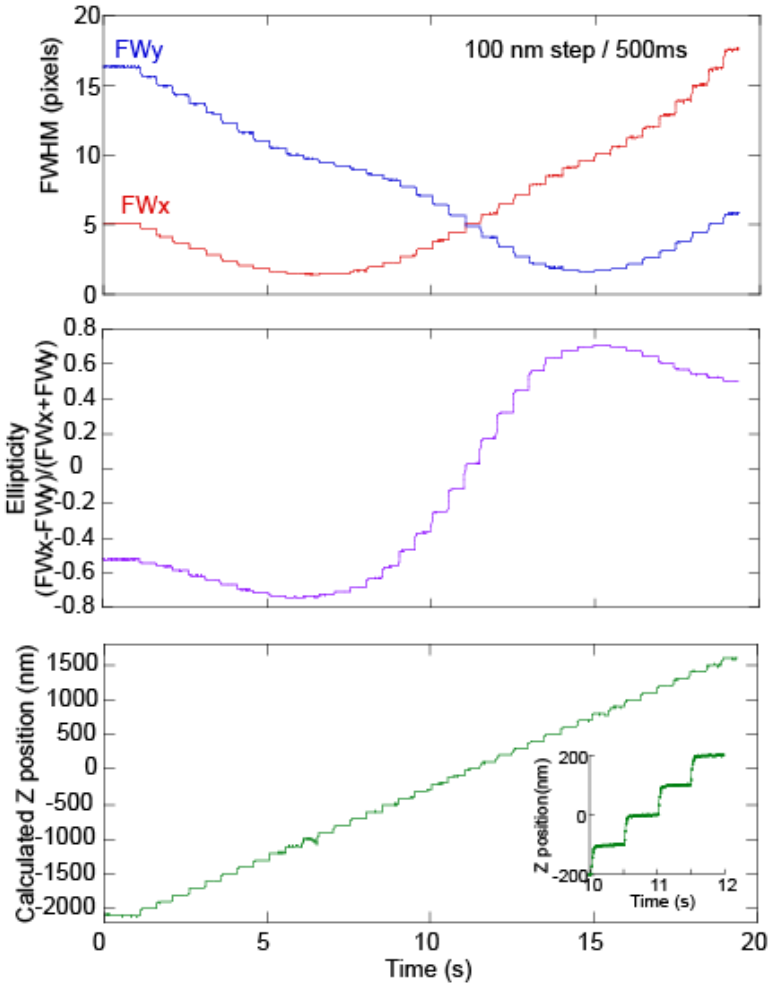

Figure S5. FWHM values of the bead images in Figure S4A in the X- (red line) and Y-axes (blue line) (upper panel), ellipticity (middle panel) and calculated positions as functions of time (lower panel). Inset shows the Z-position of the bead as a function of time. The fluorescent bead on a coverslip was moved in discrete 100 nm steps in Z-axis by a Piezo actuator with a temporal resolution of 500 ms.

SUPPLEMENTAL FIGURES S6-7

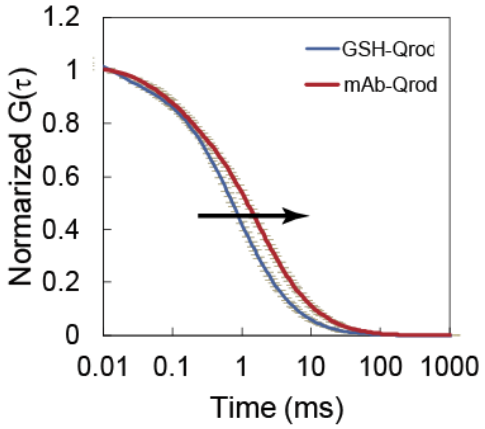

Figure S6. Autocorrelation functions of a GSH-Qrod (blue line) and a mAb-Qrod (red line). The curves and error bars represent average values and standard deviations, respectively. The arrow marks an increase in Qrod diffusion time.

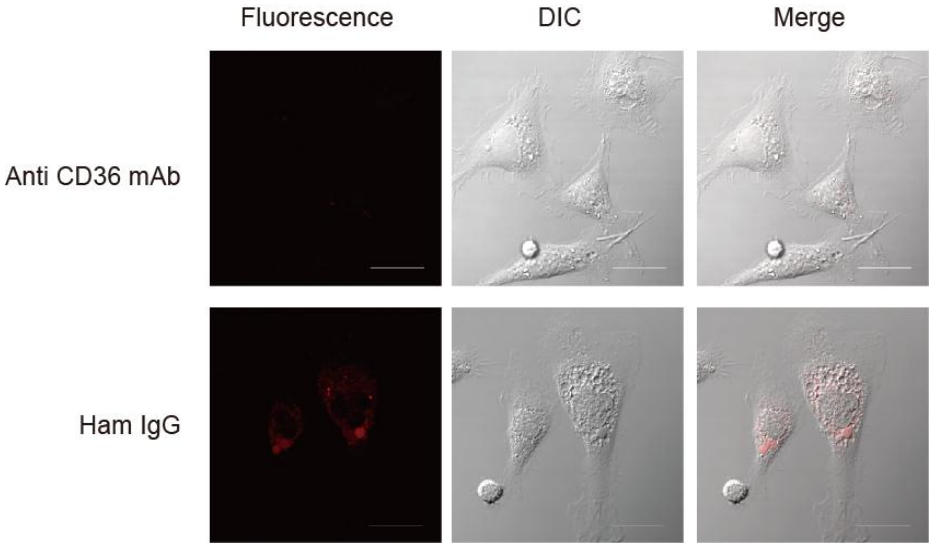

Figure S7. Blocking mAb-Qrod binding to macrophages by pretreatment with unlabeled anti-CD36 mAb. Macrophages were pretreated with anti-CD36 mAb (upper panels) or American hamster IgG (lower panels) for 1 hour, followed by incubation with mAb-Qrods. Left, middle and right columns indicate fluorescent, differential interference contrast (DIC) and merged images, respectively. Red represents mAb-Qrod signals through a band path filter (575-675 nm).

SUPPLEMENTAL FIGURES 8-11

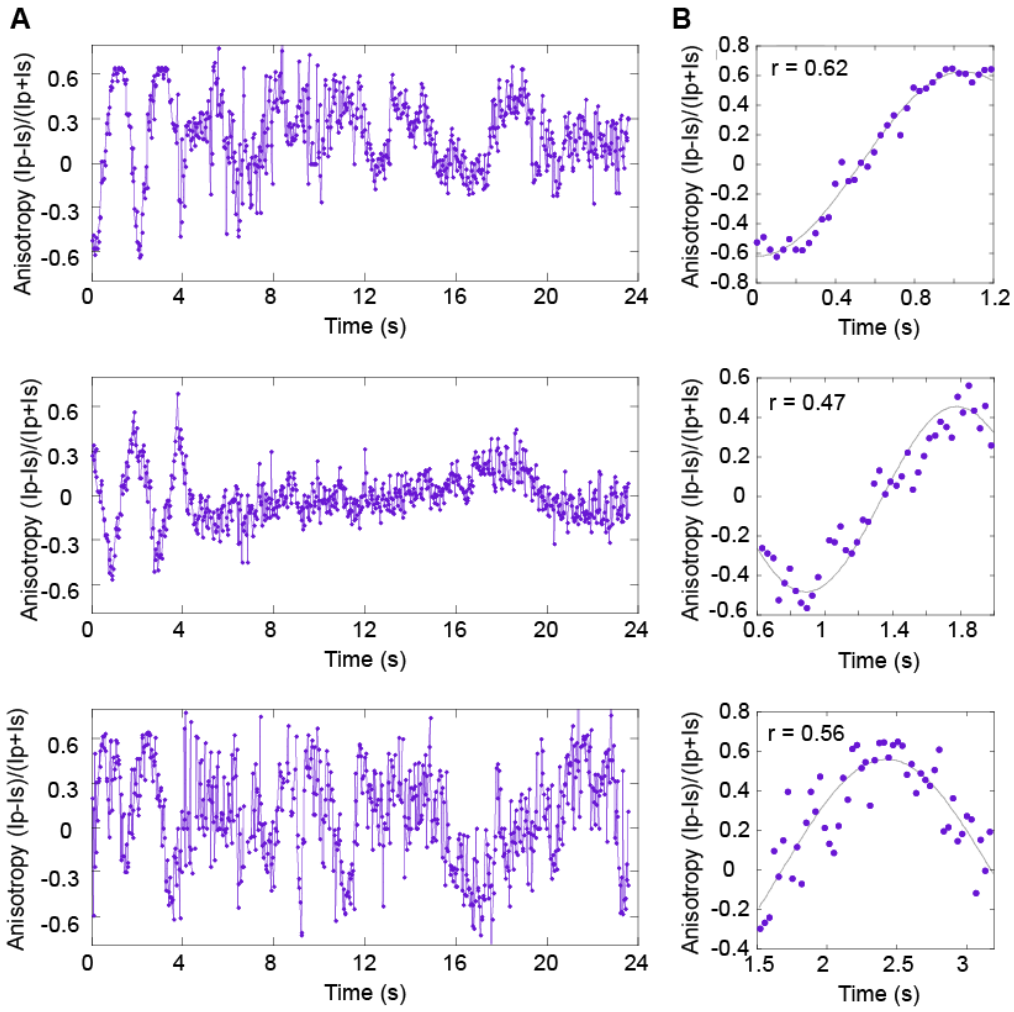

Figure S8. Angular calibration before 4D single particle tracking in macrophages. (**A**) 3 typical anisotropy traces for different mAb-Qrods in macrophages. The 1/2λ wave plate was rotated 360^{o} within the initial 4 sec among the total tracking period. (**B**) Magnified portions in **A**. Gray lines are results of fitting with a sine function (y = a_1· sin{ a_2· (x-a_3)}). We defined a_1 as the polarization factor (see main text). The parameter of a_2 would be 1/45 because the 1/2λ wave plate was rotated 360^{o} within the 4 sec (2.0×4/360). However, it is possible that a_2 slightly differed depending on the movements of Qrods.

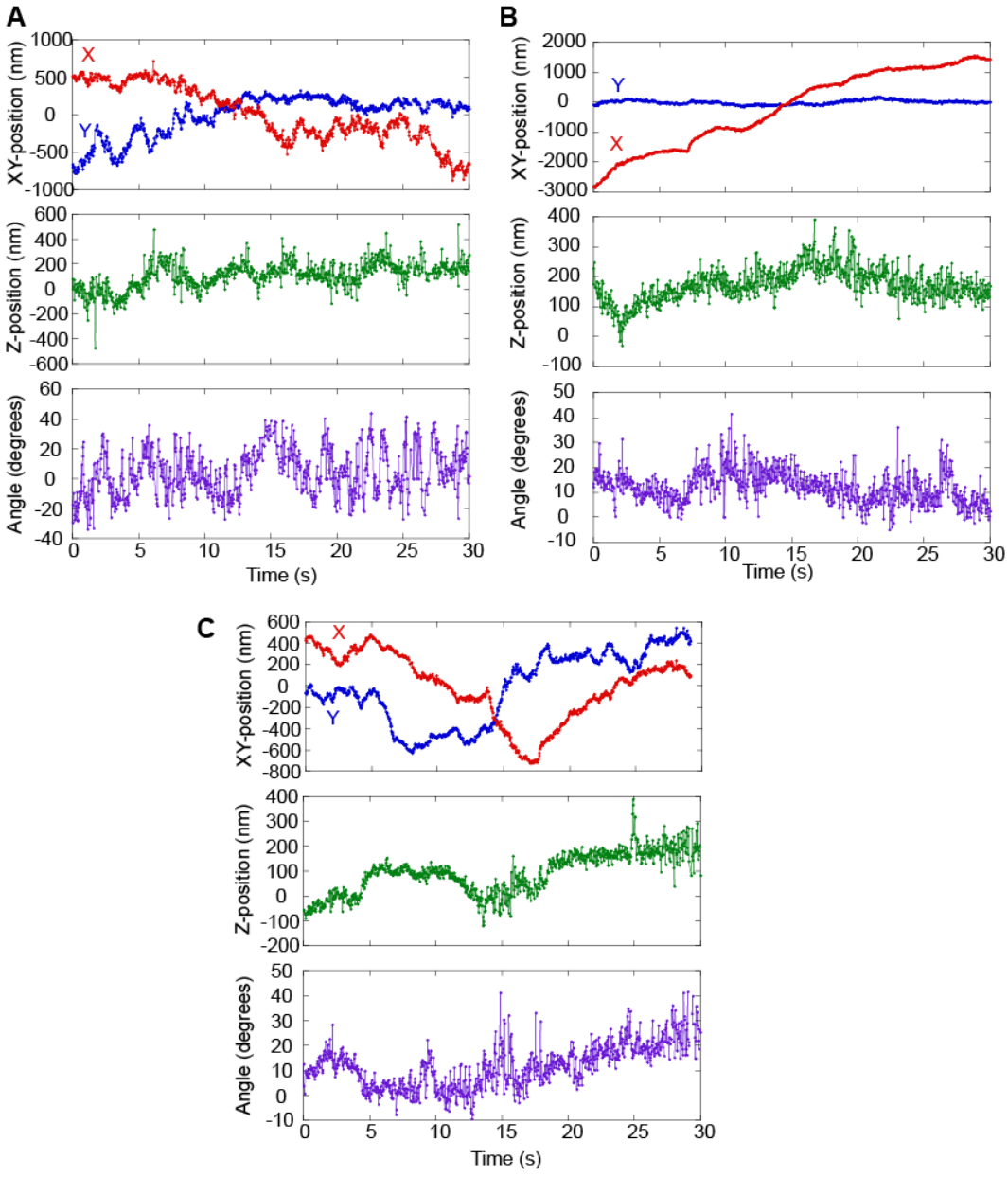

Figure S9. 4D single particle tracking of mAb-Qrods in macrophages. (**A-C**)Time courses of the X- (red line, upper panels), Y- (blue line, upper panels) and Z-axes (middle panels), and angular motion (lower panels) of the 4D trajectories shown in Figure 5 F-H, The polarization factors were 0.70 (**A**), 0.49 (**B**) and 0.64 (**C**), respectively.

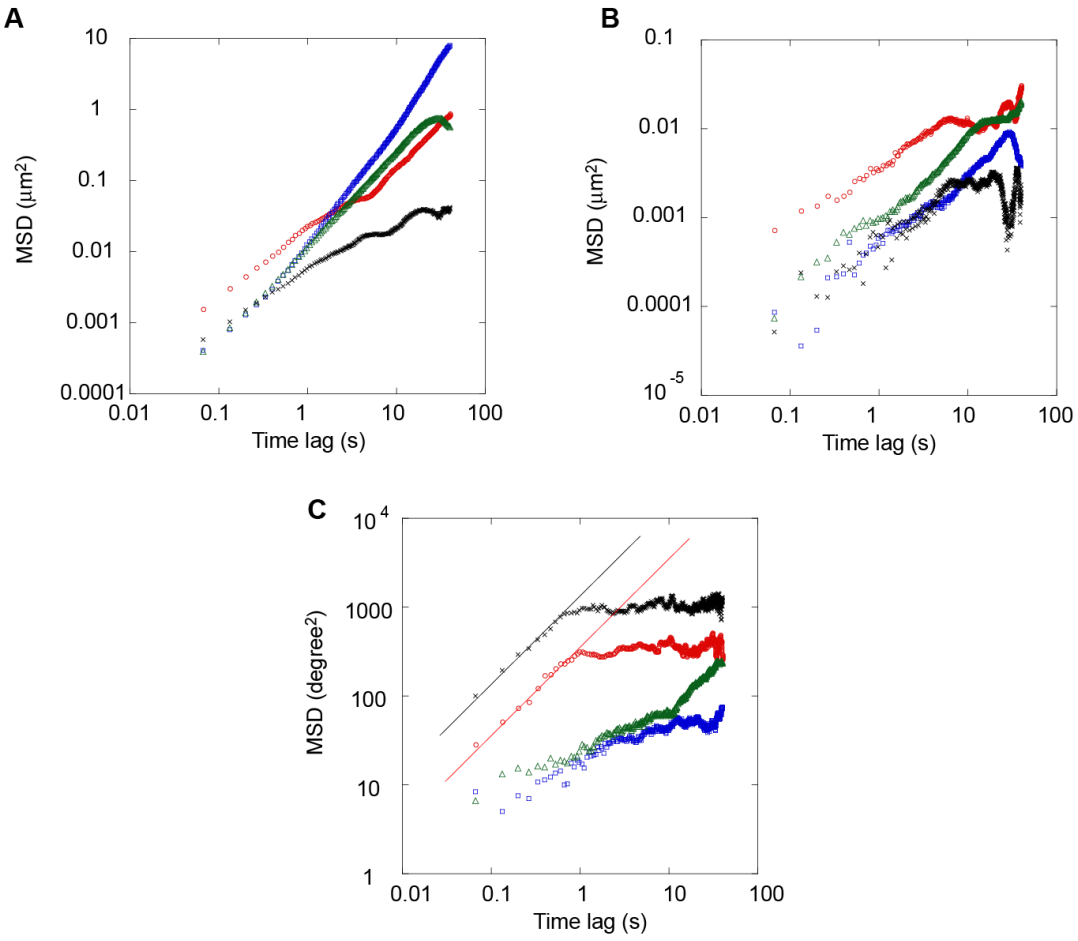

Figure S10. Mean square displacement (MSD) analysis of 4D trajectories. (**A**-**C**) Logarithmic plots of MSD in the XY-plane (**A**), Z-axis (**B**) and angular (**C**) axes of the individual mAb-Qrods shown in Figure 5 F (*red*), G (*blue*), H (*green*) and Figure S11 (*black*). MSD was calculated as (1):

$$MSD(n\delta t) = \frac{1}{N-1-n}\sum_{j=1}^{N-1-n}\{f(j\delta t + n\delta t) - f(j\delta t)\}^2, \delta t = 0.033(\text{sec})$$

where $f(j\delta t+n\delta t)$ describes the values of each axis following a time interval $n\delta t$ after starting at position $f(j\delta t)$, and N is the total number of data. The experimental obtained MSD includes random error in the determination of the position calculation, characterized by mean error σ, and is given by,

$$MSD_n(n\delta t) = MSD(n\delta t) + 2\sigma^2.$$

These plots were results that the noise was corrected by a method previously reported (2). The red and black lines in **C** are fitting results by a liner function ($f(\delta t) = 2D\cdot\delta t$) during 0.06 to 0.66 s of the time lag. The values of D were 344 (*red*) and 1278 (*black*) degrees^2/s, respectively.

1. Kusumi, A., Y. Sako, and M. Yamamoto M. 1993. *Biophys J*. 65:2021-2040.
2. Martin DS, Forstner MB, Käs JA. 2002. *Biophys J*. 83:2109-2017.

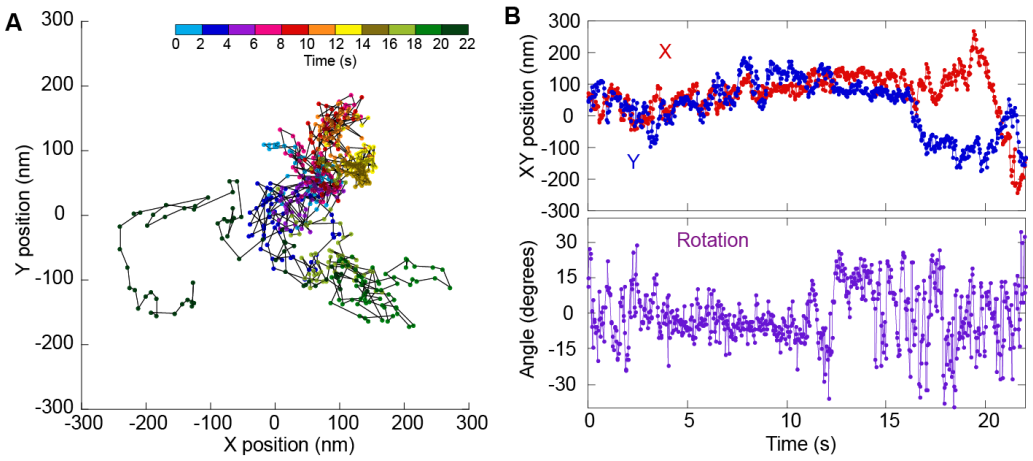

Figure S11. Relationship between lateral and angular movement of mAb-Qrods on the cell membrane. (**A**) A typical 2D trace of free diffusion of mAb-Qrods on the cell membrane. Color indicates running time. (**B**) Time courses of each axis in trace **A**. Red, X; Blue, Y; Magenta, angle.